

Chain-Shortened Myostatin Inhibitory Peptides Improve Grip Strength in Mice

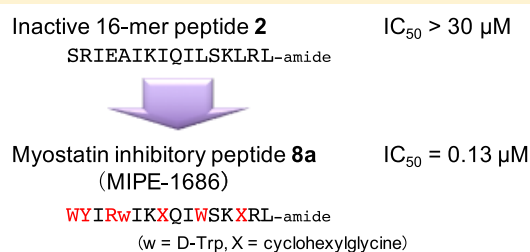
Kentaro Takayama,[†] Tomo Asari,[†] Mariko Saitoh,[†] Kei Nirasawa,[§] Eri Sasaki,[§] Yoshimi Roppongi,[†] Akari Nakamura,[†] Yusuke Saga,[†] Takahiro Shimada,[†] Hiroaki Ikegama,[†] Akihiro Taguchi,[†] Atsuhiko Taniguchi,[†] Yoichi Negishi,[§] and Yoshio Hayashi^{*,†,‡}

[†]Department of Medicinal Chemistry and [§]Department of Drug Delivery and Molecular Biopharmaceutics, Tokyo University of Pharmacy and Life Sciences, Hachioji, Tokyo 192-0392, Japan

S Supporting Information

ABSTRACT: Inhibition of myostatin is a promising strategy for treatment of muscle atrophic disorders. We had already identified a 23-mer peptide (**1**) as a synthetic myostatin inhibitor, and structure–activity relationship studies with **1** afforded a potent 22-mer peptide derivative (**3**). Herein, we report the shortest myostatin inhibitory peptide so far. Among chain-shortened 16-mer peptidic inhibitors derived from the C-terminal region of **3**, peptide inhibitor **8a** with β -sheet propensity was twice as potent as 22-mer inhibitor **3** and significantly increased not only muscle mass but also hind limb grip strength in Duchenne muscular dystrophic model mice. These results suggest that **8a** is a promising platform for drug development treating muscle atrophic disorders.

KEYWORDS: Inhibitor, peptide, muscle atrophic disorder, myostatin, structure–activity relationship



Myostatin, a negative regulatory factor of muscle growth categorized as a member of the transforming growth factor- β (TGF- β) superfamily,¹ is a promising target for muscle atrophic disorders, including muscular dystrophy, sarcopenia, and cachexia. During the last two decades, several strategies for myostatin inhibition have been reported. In 2002, Bogdanovich et al. reported that an antimyostatin antibody improved muscle mass and strength in Duchenne muscular dystrophic (DMD) model mice.² Recently, Andre et al. reported that a mouse antimyostatin antibody and its humanized analogue “domagrozumab (mRK35)” induced skeletal muscle hypertrophy in both *mdx* mice and cynomolgus monkeys.³ In 2010, an antibody Fc fragment-fused soluble decoy of activin type II receptor was reported as a myostatin inhibitor, which improved cachexia symptom in tumor-bearing mice.⁴ Other myostatin inhibitory strategies including antibodies are currently in clinical trials against muscle atrophic diseases,^{5,6} although some failures have been reported.^{7,8} Mariot et al. suggested the importance of patient selection and stratification in future clinical trials regarding antimyostatin approach.⁹ Proteins related to the myostatin prodomain and follistatin, whose binding modes with myostatin have been determined by X-ray crystal structural analysis,^{10–16} are also myostatin-inactivating proteins. Jiang et al. reported an inhibitory-core 74 amino acid fragment derived from the N-terminal region (positions: 19–92) of the human myostatin prodomain protein, which exhibits antimyostatin activity as a glutathione S transferase-fusion protein.¹⁰

In contrast to these protein-based inhibitors, we recently identified peptide-based inhibitors (23/29-mer) from positions

21–43/19–47 of the mouse myostatin prodomain, which were easily and inexpensively synthesized by general Fmoc-based solid phase chemistry.^{17,18} We carried out structure–activity relationship (SAR) studies based on peptide **1** (peptide **7** in ref 18) whose IC₅₀ is 3.56 μ M, with a minimum sequence composed of 23 amino acid residues (positions: 21–43) and, as a result, obtained a potent 22-mer peptide derivative **3** (XRQNTYRSRIEWIKIQLSKLRL–amide, X = 2-naphthyloxycetyl, peptide **3d** in ref 21) whose IC₅₀ is 0.32 μ M.^{18–21} Peptide **3** increases muscular mass in both the DMD-model *mdx* and wild-type mice.²¹ In an alternative SAR study, we identified residues important for effective myostatin inhibition by Ala-scanning of peptide **1**. The important residues were Trp21, Tyr27, Ile30, Ile33, Ile35, Ile37, Leu38, Leu41, and Leu43.¹⁹

In peptide drug development, reduction of peptide-size is a very important priority because it is generally expected to result in decreasing antigenicity, increasing in vivo stability, and reducing production cost.²² Our previously synthesized chain-shortened peptide **2** (Figure 1A; positions: 28–43; 16-mer; peptide **11** in ref 18), however, failed to show inhibitory activity at a concentration of 30 μ M, despite including all the important branched-chain residues (Ile and Leu) mentioned above.¹⁹ This result suggests that an appropriately recon-

Received: April 15, 2019

Accepted: May 28, 2019

Published: May 28, 2019



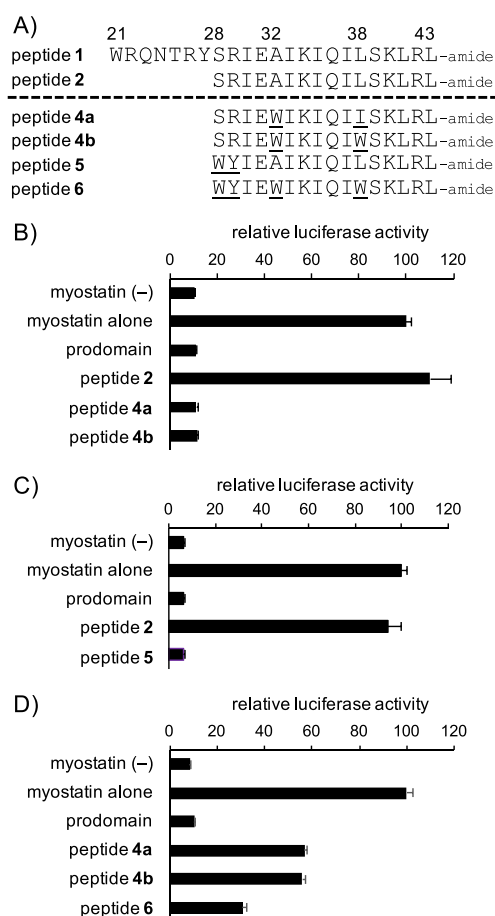


Figure 1. (A) Sequences of previously reported peptides 1–2¹⁸ and newly synthesized peptides 4a, 4b, 5, and 6. The numbers above each amino acid indicate the position in the prodomain sequence of mouse myostatin. (B–D) Luciferase reporter assay experiments determined the activities of peptides 4a, 4b, 5, and 6 toward myostatin inhibition. Peptide concentration: 10 (B,C) and 3 μ M (D). Results are presented as mean values \pm SD ($n = 3$).

structured interaction with myostatin should be considered in the design of inhibitory peptides.

Consequently, in the present study, we designed and synthesized a series of chain-shortened peptides based on peptide 3 in an effort to optimize its interaction with myostatin, changing the amino acid residues to those possessing more appropriate side chain structures using natural or unnatural amino acids. From an SAR study of these peptides, a new potent 16-mer peptide inhibitor 8a was discovered and was found to be able to significantly increase not only muscle mass but also grip strength in *mdx* mice.

In this study, all peptides assessed were prepared by a Fmoc-based solid-phase peptide synthesis using an SAL amide resin in an automatic peptide synthesizer as described in the Supporting Information. Briefly, a coupling reaction of each protected amino acid residue was performed using a HATU/HOAt/DIEA system after deprotection of the N-terminal Fmoc group with 20% piperidine in DMF. The crude peptide was obtained from constructed protected peptide resin by final deprotection using a TFA/*m*-cresol/thioanisole/EDT system. The resulting crude peptides were purified by preparative reversed-phase high-performance liquid chromatography (RP-HPLC), and the purified peptides all displayed a purity of

>95% in analytical RP-HPLC (see Supporting Information). All the synthetic peptides were characterized by electrospray ionization time-of-flight mass spectrometry (see Supporting Information). A 3 mM stock solution of each peptide in DMSO was prepared for *in vitro* bioassay.

The *in vitro* myostatin inhibitory activities of all peptide derivatives were evaluated by a luciferase reporter assay using HEK293 cells (see Supporting Information). In our previous report, the respective substitutions to Trp and Ile/Trp residues at positions 32 and 38 in peptide 1 could improve the inhibitory activity as seen in peptide 3,²¹ while chain-shortened peptide 2 derived from peptide 1 was inactive.¹⁸ Therefore, in the present study, we applied the same Ile/Trp substitutions to inactive peptide 2. The corresponding peptides 4a and 4b were synthesized (Figure 1A), and their inhibitory activity was evaluated. Surprisingly, as shown in Figure 1B, the effective myostatin inhibitory activity of 16-mer peptides 4a and 4b was observed at a concentration of 10 μ M, while no myostatin inhibitory activity was reproduced with the 16-mer peptide 2, which had previously been reported to be inactive.¹⁸ The inhibitory potency of peptides 4a (Ile38) and 4b (Trp38) at a concentration of 3 μ M was almost equivalent as shown in Figure 1D. This was the first discovery of chain-shortened 16-mer peptides (MIPE-16) with significant myostatin inhibitory activity, and indicated that introduction of amino acid residues possessing appropriate hydrophobic side chains can be equivalent to shortening inhibitory peptides by as many as six residues. Compared to the conservative substitution of Leu to Ile at position 38, substitution from Ala for Trp at position 32, i.e., introduction of an indole structure, probably had a great impact in development of a new hydrophobic interaction to myostatin. These two substitutions have a large impact on the activity because the chain-shortened peptides 4a and 4b possess the effective inhibitory activity, although they lack important residues Trp21 and Tyr27 at the N-terminal part of peptide 1 as mentioned above.¹⁹

As an alternative approach, since Ser28 and Arg29 were thought to be unimportant residues in the Ala scanning of peptide 1,¹⁹ the two corresponding residues in the inactive chain-shortened peptide 2 were substituted to the aforementioned important residues Trp and Tyr, respectively. Peptide 5 was synthesized (Figure 1A) and its inhibitory activity was evaluated. Interestingly, the peptide 5 exhibited effective myostatin inhibitory activity at a concentration of 10 μ M (Figure 1C).

Encouraged by these breakthrough results, we tried to combine these two findings. We synthesized peptide 6 (Figure 1A) with Trp28, Tyr29, Trp32, and Trp38 and evaluated its myostatin inhibitory activity. At a more diluted concentration of 3 μ M, peptide 6 displayed a more potent inhibitory activity than peptides 4a and 4b (Figure 1D). This result suggests that each hydrophobic side chain structure appropriately interacts with myostatin. Consequently, we successfully obtained a potent chain-shortened (16-mer) myostatin inhibitor 6 as a new lead for further SAR study and structural optimization.

In the first step of the SAR study based on peptide 6, we focused on the acidic Glu31 residue, which is one of the unimportant residues identified by the Ala scanning study,¹⁹ and synthesized four derivatives (E31K, E31R, E31N, and E31Q) as shown in Figure 2A. This position has not been modified in our previous SAR study. Among the four compounds, E31R at an even more diluted concentration of 0.3 μ M showed the most improved activity over that of 6

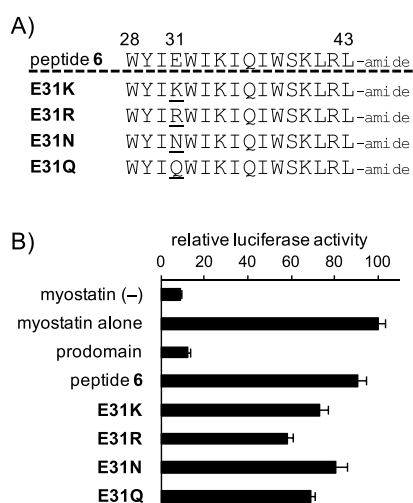


Figure 2. (A) Sequences of the Glu-substituted peptides. The numbers above each amino acid indicate its position in the prodomain sequence of mouse myostatin. (B) Luciferase reporter assay to determine the activities of the Glu-substituted peptides toward myostatin inhibition, relative to peptide 6. Peptide concentration: 0.3 μ M. Results are presented as mean values \pm SD ($n = 3$).

(Figure 2B). Therefore, we examined the *in vivo* efficacy of E31R in *mdx* mice (5-week-old male) through histological analysis based on hematoxylin and eosin staining using a previously reported procedure.²¹ As shown in Figure S1, intramuscularly injected E31R, compared to saline, induced an increase of gastrocnemius (GAS) muscle fiber sizes. Additionally, peptides 3 and E31R similarly increased GAS muscle fiber sizes in wild-type C57BL/6 mice compared to saline (Figure S2). These results suggest that the shortened peptide E31R (16-mer) also functions as a myostatin inhibitor, leading to induction of muscular hypertrophy in mice.

Introduction of unnatural amino acids into bioactive peptides is a useful strategy to increase the diversity of the peptide structures that lead to the potential interaction with the clinical target and the enhanced stability against degradation *in vivo*.²³ From this standpoint, as one of the SAR studies based on peptide 1, we synthesized a series of peptide derivatives bearing a hydrophobic unnatural amino acid surrogate commonly used for such SAR study, cyclohexylglycine (Chg) or phenylglycine (Phg), in the positions of respective aliphatic Ile or Leu residues (Ile30, Ile33, Ile35, Ile37, Leu38, Leu41, and Leu43) (Figure S3A,C). Among the peptides substituted at Ile residues, I35Chg having the same β -blanched structure as Ile showed the most potent inhibitory activity compared to 1 and other peptides substituted by the Chg or Phg residue (Figure S3B). Among peptides substituted at Leu residues, L38Chg and L41Chg showed a stronger inhibitory activity than 1 and other substituted peptides (Figure S3D). These results suggested that Chg at position 35, 38, or 41 contributes to the increase in the inhibitory activity.

An alternative strategy to increase inhibition of the target molecule and prevent degradation *in vivo* is to introduce the D-isomers of amino acids. We carried out D-form scanning in peptide 1, especially focused on C-terminal positions 28–43, which is corresponding to the chain-shortened sequence. To do this, we synthesized 16 kinds of peptide derivative substituted to the corresponding D-form of amino acid

(lower case letter) at specific residues from position 28 to 43 (Figure S4A) and evaluated their myostatin inhibitory activities at a concentration of 3 μ M (Figure S4B). As a result, two derivatives with D-substitutions, A32a and S39s, showed improved inhibitory activities.

Based on the data in Figure S3, we conducted structural optimization of an inhibitory peptide derived from the chain-shortened peptide E31R (16-mer, Figure 2). As shown in Figure 1 and in our previous SAR study,¹⁶ it is known that Ile and Trp are also favored amino acid residues at position 38 for effective inhibition of myostatin.²¹ Therefore, we focused on the change to Chg at positions 35 and 41 in E31R and synthesized monosubstituted (7a and 7b) and disubstituted (7c) peptides (Figure 3A). In addition to these peptides, since

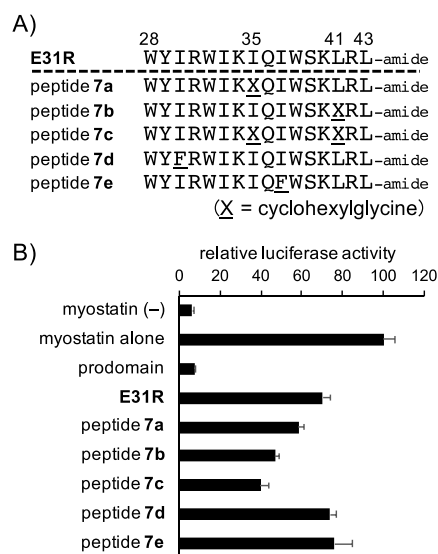


Figure 3. (A) Sequences of peptides 7a–e. The numbers above each amino acid indicate the position in the prodomain sequence of mouse myostatin. X = cyclohexylglycine (Chg). (B) Luciferase reporter assay experiments determined the activities of peptides 7a–e toward myostatin inhibition relative to E31R. Peptide concentration: 0.3 μ M. Results are presented as mean values \pm SD ($n = 3$).

substitutions I30F and I37F in peptide 1 showed an inhibitory activity similar to that of 1,²¹ we synthesized the corresponding E31R derivatives 7d (I30F) and 7e (I37F) to examine the applicability of these substitutions (Figure 3A). As a result, the Chg-incorporated peptides 7a–c showed more potent inhibitory activity than E31R, and the disubstituted 7c showed the strongest inhibitory activity (Figure 3B). However, peptides 7d and 7e exhibited a similar inhibitory activity toward E31R at a concentration of 0.3 μ M (Figure 3B). These results indicate that the effective substitutions for the inhibitory activity observed in peptide 1 (23-mer) can be reflected in the chain-shortened peptides, suggesting that the chain-shortened peptides interact with myostatin in the same manner as peptide 1-derivatives. Consequently, introduction of unnatural amino acid residue into the chain-shortened peptide effectively improved the inhibitory activity.

Finally, we applied the result of this D-form scanning shown in Figure S4 to the chain-shortened peptide 7c (16-mer), and its derivatives 8a–c (Figure 4A) were synthesized. Interestingly, only peptide 8a (W32w) exhibited the enhanced activity compared to 7c, while the inhibitory activity of 8b (S39s) was

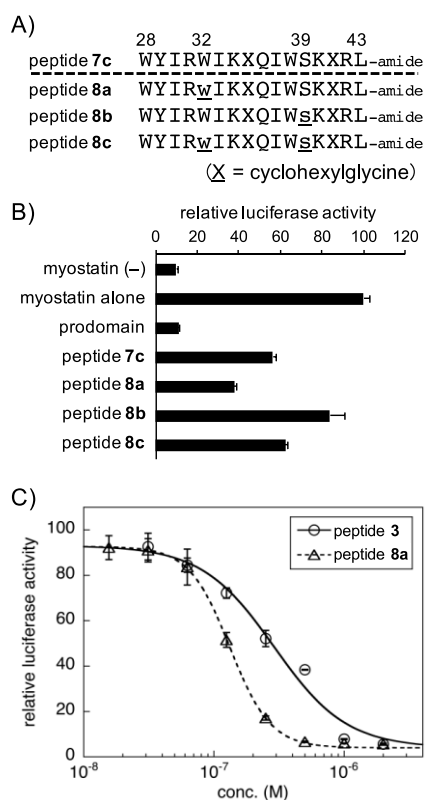
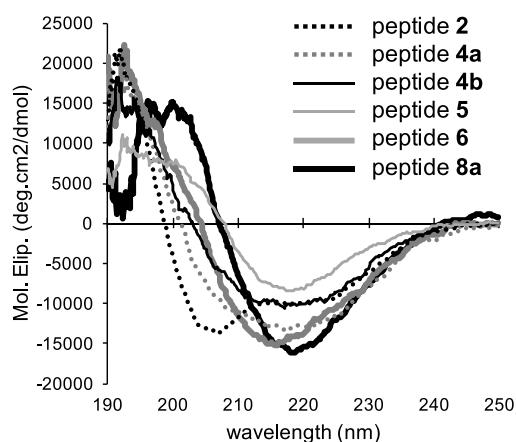


Figure 4. (A) Sequences of peptides 8a–c. The numbers above each amino acid indicate the position in the prodomain sequence of mouse myostatin. X = cyclohexylglycine (Chg). Lower case letter = D-form of the amino acid. (B) Luciferase reporter assay experiments determined the activities of peptides 8a–c in myostatin inhibition relative to peptide 7c. Peptide concentration: 0.3 μ M. Results are presented as mean values \pm SD ($n = 3$). (C) Dose-dependent myostatin inhibitory activities of peptides 3 and 8a at concentrations of 0.032–2 and 0.016–2 μ M, respectively. Results are presented as mean values \pm SD ($n = 3$). Curve fitting was performed using KaleidaGraph 4.5.

diminished and the double-substituted derivative 8c (W32w, S39s) retained the activity (Figure 4B). These results indicated that the W32w substitution enhanced the activity, although its effect was canceled by the S39s substitution.

To compare the inhibitory activity of the most potent chain-shortened peptide 8a (16-mer) with the known 22-mer peptide (3), a dose-dependency study was performed at peptide concentrations ranging from 0.016 to 2 μ M (peptide 3, 0.032–2 μ M; peptide 8a, 0.016–2 μ M) (Figure 4C). The IC_{50} values of peptides 3 and 8a were 0.29 ± 0.05 and 0.13 ± 0.002 μ M, respectively. This result indicates that peptide 8a, in spite of six-residue shortening, is twice as potent a myostatin inhibitor than the known structurally optimized 22-mer peptide 3.

To understand the secondary structure of chain-shortened peptides, circular dichroic (CD) spectra of representative peptides 2, 4a, 4b, 5, 6, and 8a were measured and analyzed by the previously reported method (Figure 5).^{18,24} In our previous reports, peptide 1 showed a tendency to form α -helix structure (α -helix, 45%; β -sheet, 5%; turn, 14%; random coil, 36%), while peptide 3 displayed the propensity to form β -sheet structure (α -helix, 8%; β -sheet, 58%; turn, 0%; random coil, 34%).²⁴ As shown in Figure 5, inactive peptide 2, the N-terminal truncated form of peptide 1, retained α -helical



structural content (%)	peptide					
	2	4a	4b	5	6	8a
α -helix	31	21	11	0	10	0
β -sheet	18	46	58	64	60	76
turn	10	0	0	4	0	0
random coil	41	33	31	32	30	24

Figure 5. CD spectra of peptides 2, 4a, 4b, 5, 6, and 8a in 20 mM sodium phosphate buffer (pH 7.4) containing 10% 2,2,2-trifluoroethanol; peptide concentration, 5 μ M. CD spectra were analyzed by using Jasco secondary estimation software with Reed's reference set as reference spectra.

characteristics of 1, although the proportion of random coil structure content to α -helix content was slightly increased compared with that of 1.²⁴ Inhibitory peptide 4a, the N-terminal truncated form of peptide 3, showed relatively higher content of β -sheet structure (46%) than α -helix content (21%). These results suggested that the myostatin inhibitory activity of peptide 4a is attributed to the adequate hydrophobic interaction derived from its β -sheet structure, predominantly formed by amino acid substitutions at positions 32 and 38, which is a similar case previously observed in peptide 3.²¹ Compared with peptide 4a, other inhibitory peptides 4b, 5, 6, and 8a exhibited even higher content of the β -sheet structure along with their enhanced inhibitory activity (Figure 5). In particular, the content of the most potent peptide 8a was 76%. Therefore, the results imply that the β -sheet propensity in the peptide secondary structure is one of the important factors for enhancing myostatin inhibition. Elucidation of these precise molecular interactions between myostatin and inhibitory peptides with β -sheet propensity would be a challenging but significant work in the future.

To investigate the effect of peptide 8a *in vivo*, as reported previously,¹⁸ a saline solution of 8a (30 nmol) or saline was injected into the tibialis anterior (TA) muscle of *mdx* mice (5-week-old males) at days 0 and 14. Then, at day 42, the treated TA muscles were collected and weighed. Peptide 8a significantly increased the weight of TA muscles to $114 \pm 6.6\%$ compared with saline-treated muscles (Figures 6A and S5). Moreover, to understand the improvement of muscle function following treatment with peptide 8a, the grip strength of hind limb at day 42 was measured. Peptide 8a (30 nmol) or

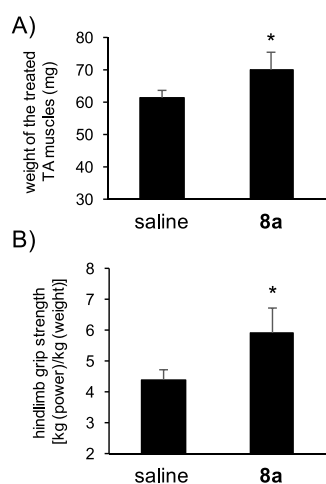


Figure 6. (A) Weight of tibialis anterior (TA) muscles in *mdx* mice treated with peptide **8a** (left) or the vehicle (saline, right). Forty microliters of a 0.75 mM solution of peptide **8a** in saline was intramuscularly injected into the tibialis anterior muscle of *mdx* mice. Treatment was repeated 2 weeks later in the same muscle. The muscles were collected and weighed 4 weeks after the last treatment ($n = 4$). Results are presented as mean values \pm SD ($n = 4$). (B) Grip strength of hind limb treated with peptide **8a** in saline. Forty microliters of the peptide solution (0.75 mM peptide **8a** in saline) was injected intramuscularly into four points in each leg of *mdx* mice at days 0 and 14. The values of hind limb grip strength at day 42 are presented as mean values \pm SD ($n = 4$). * $p < 0.05$.

saline was intramuscularly injected into four points of *mdx* mice at days 0 and 14. The hind limb grip strength (kg) per body weight (kg) in peptide **8a** or saline-treated mice at day 42 was 5.92 ± 0.82 and 4.41 ± 0.31 , respectively (Figure 6B), indicating that peptide **8a** significantly improved muscle function to about 130%. This result suggests that peptide **8a** functions as a muscle enhancer through myostatin inhibition. Although it has already been known that inhibitors of myostatin and its antibodies generally act as muscle enhancers,^{2–8,10–13} easily synthesized peptide **8a** is currently the smallest peptide known to have this effect. This finding probably could serve as a promising milestone in peptide-based drug development.

In this study, we successfully discovered chain-shortened 16-mer inhibitory peptides against myostatin (MIPE-16). As is the case with peptide **3**, **E31R**, composed of only natural amino acids, induces muscular hypertrophy in pathological *mdx* and wildtype C57BL/6 mice. The most potent 16-mer peptide in this study (**8a**, designated as MIPE-1686), which contains the unnatural amino acids Chg and D-Trp, shows twice more potent inhibitory activity *in vitro* than 22-mer peptide **3**. In a study using *mdx* mice, peptide **8a** (MIPE-1686) significantly improved the weight of tibialis anterior muscle and the hindlimb grip strength. This is a first report that myostatin inhibitory peptides composed of less than 20 amino acids show functional improvement of skeletal muscle in pathological model mice. The chain-shortened myostatin inhibitory peptide **8a** (MIPE-1686) could be a promising lead for drug development of inhibitors of muscle atrophic disorders.

■ ASSOCIATED CONTENT

Supporting Information

The Supporting Information is available free of charge on the ACS Publications website at DOI: 10.1021/acsmmedchemlett.9b00174.

Materials, experimental procedure, analytical data for all peptide derivatives, analytical HPLC chromatograms, Figures S1–S5 (PDF)

■ AUTHOR INFORMATION

Corresponding Author

*Tel/Fax: +81 42 676 3275. E-mail: yhayashi@toyaku.ac.jp.

ORCID

Yoshio Hayashi: 0000-0002-7010-6914

Author Contributions

The manuscript was written through contributions of all authors. All authors have given approval to the final version of the manuscript.

Funding

This research was supported by the Japan Society for the Promotion of Sciences (JSPS) KAKENHI, including Grants-in-Aid for Scientific Research (B) 15H04658 (to K.T. and Y.H.), MEXT-supported Program for the Strategic Research Foundation at Private Universities, and Intramural Research Grant (29-4) for Neurological and Psychiatric Disorders on NCNP (to Y.H.).

Notes

The authors declare no competing financial interest.

■ ACKNOWLEDGMENTS

The authors thank Mr. Shota Takayama for peptide synthesis.

■ ABBREVIATIONS

CD, circular dichroism; Chg, cyclohexylglycine; DIEA, *N,N'*-diisopropylethylamine; DMD, Duchenne muscular dystrophy; DMSO, dimethyl sulfoxide; Fmoc, 9-fluorenylmethoxycarbonyl; GAS, gastrocnemius; HATU, *O*-(7-aza-1*H*-benzotriazol-1-yl)-*N,N,N',N'*-tetramethyluronium hexafluorophosphate; HEK293, human embryonic kidney 293; HOAt, 1-hydroxy-7-azabenzotriazole; MIPE-16, 16-mer myostatin inhibitory peptides; Phg, phenylglycine; SAR, structure–activity relationship; TA, tibialis anterior; TGF- β , transforming growth factor- β

■ REFERENCES

- (1) McPherron, A. C.; Lawler, A. M.; Lee, S.-J. Regulation of skeletal muscle in mice by a new TGF- β superfamily member. *Nature* **1997**, *387*, 83–90.
- (2) Bogdanovich, S.; Krag, T. O.; Barton, E. R.; Morris, L. D.; Whittemore, L. A.; Ahima, R. S.; Khurans, T. S. Functional improvement of dystrophic muscle by myostatin blockade. *Nature* **2002**, *420*, 418–421.
- (3) St Andre, M.; Johnson, M.; Bansal, P. N.; Wellen, J.; Robertson, A.; Opsahl, A.; Burch, P. M.; Bialek, P.; Morris, C.; Owens, J. A mouse anti-myostatin antibody increases muscle mass and improves muscle strength and contractility in the *mdx* mouse model of Duchenne muscular dystrophy and its humanized equivalent, domagrozumab (PF-06252616), increases muscle volume in cynomolgus monkeys. *Skelet. Muscle* **2017**, *7*, 25.
- (4) Zhou, X.; Wang, J. L.; Lu, J.; Song, Y.; Kwak, K. S.; Jiao, Q.; Rosenfeld, R.; Chen, Q.; Boone, T.; Scott Simonet, W.; Lacey, D. L.; Goldberg, A. L.; Han, H. Q. Reversal of cancer cachexia and muscle

wasting by ActRIIB antagonism leads to prolonged survival. *Cell* **2010**, *142*, 531–543.

(5) Becker, C.; Lord, S. R.; Studenski, S. A.; Warden, S. J.; Fielding, R. A.; Recknor, C. P.; Hochberg, M. C.; Ferrari, S. L.; Blain, H.; Binder, E. F.; Rolland, Y.; Poiraudou, S.; Benson, C. T.; Myers, S. L.; Hu, L.; Ahmad, Q. I.; Pacuch, K. R.; Gomez, E. V.; Benichou, O. Myostatin antibody (LY2495655) in older weak fallers: a proof-of-concept, randomised, phase 2 trial. *Lancet Diabetes Endocrinol.* **2015**, *3*, 948–957.

(6) Glasser, C. E.; Gartner, M. R.; Wilson, D.; Miller, B.; Sherman, M. L.; Attie, K. M. Locally acting ACE-083 increases muscle volume in healthy volunteers. *Muscle Nerve* **2018**, *57*, 921–926.

(7) Campbell, C.; McMillan, H. J.; Mah, J. K.; Tarnopolsky, M.; Selby, K.; McClure, T.; Wilson, D. M.; Sherman, M. L.; Escobar, D.; Attie, K. M. Myostatin inhibitor ACE-031 treatment of ambulatory boys with Duchenne muscular dystrophy: Results of a randomized, placebo-controlled clinical trial. *Muscle Nerve* **2017**, *55*, 458–464.

(8) Golan, T.; Geva, R.; Richards, D.; Madhusudan, S.; Lin, B. K.; Wang, H. T.; Walgren, R. A.; Stemmer, S. M. LY2495655, an antimyostatin antibody, in pancreatic cancer: a randomized, phase 2 trial. *J. Cachexia Sarcopenia Muscle* **2018**, *9*, 871–879.

(9) Mariot, V.; Joubert, R.; Hourde, C.; Féasson, L.; Hanna, M.; Muntoni, F.; Maissonobe, T.; Servais, L.; Bogni, C.; Le Panse, R.; Benvensite, O.; Stojkovic, T.; Machado, P. M.; Voit, T.; Buj-Bello, A.; Dumonceaux, J. Downregulation of myostatin pathway in neuro-muscular diseases may explain challenges of anti-myostatin therapeutic approaches. *Nat. Commun.* **2017**, *8*, 1859.

(10) Jiang, M.-S.; Liang, L.; Wang, S.; Ratovitski, T.; Holmstrom, J.; Barker, C.; Stotish, R. Characterization and identification of the inhibitory domain of GDF-8 propeptide. *Biochem. Biophys. Res. Commun.* **2004**, *315*, 525–531.

(11) Hill, J. J.; Davies, M. V.; Pearson, A. A.; Wang, J. W.; Hewick, R. M.; Wolfman, N. M.; Qiu, Y. The myostatin propeptide and the follistatin-related gene are inhibitory binding proteins of myostatin in normal serum. *J. Biol. Chem.* **2002**, *277*, 40735–40741.

(12) Lee, Y.-S.; Lee, S.-J.; Zimmers, T. A.; Soleimani, A.; Matzuk, M. M.; Tsuchida, K.; Cohn, R. D.; Barton, E. R. Regulation of muscle mass by follistatin and activins. *Mol. Endocrinol.* **2010**, *24*, 1998–2008.

(13) Nakatani, M.; Takehara, Y.; Sugino, H.; Matsumoto, M.; Hashimoto, O.; Hasegawa, Y.; Murakami, T.; Uezumi, A.; Takeda, S.; Noji, S.; Sunada, Y.; Tsuchida, K. Transgenic expression of a myostatin inhibitor derived from follistatin increases skeletal muscle mass and ameliorates dystrophic pathology in mdx mice. *FASEB J.* **2008**, *22*, 477–487.

(14) Cash, J. N.; Rejon, C. A.; McPherron, A. C.; Bernard, D. J.; Thompson, T. B. The structure of myostatin:follistatin 288: insights into receptor utilization and heparin binding. *EMBO J.* **2009**, *28*, 2662–2676.

(15) Cash, J. N.; Angerman, E. B.; Kattamuri, C.; Nolan, K.; Zhao, H.; Sidis, Y.; Keutmann, H. T.; Thompson, T. B. Structure of myostatin-follistatin-like 3: N-terminal domains of follistatin-type molecules exhibit alternate modes of binding. *J. Biol. Chem.* **2012**, *287*, 1043–1053.

(16) Cotton, T. R.; Fischer, G.; Wang, X.; McCoy, J. C.; Czepnik, M.; Thompson, T. B.; Hyvönen, M. Structure of the human myostatin precursor and determinants of growth factor latency. *EMBO J.* **2018**, *37*, 367–383.

(17) Ohsawa, Y.; Takayama, K.; Nishimatsu, S.; Okada, T.; Fujino, M.; Fukai, Y.; Murakami, T.; Hagiwara, H.; Itoh, F.; Tsuchida, K.; Hayashi, Y.; Sunada, Y. The inhibitory core of the myostatin prodomain: its interaction with both type I and II membrane receptors, and potential to treat muscle atrophy. *PLoS One* **2015**, *10*, No. e0133713.

(18) Takayama, K.; Noguchi, Y.; Aoki, S.; Takayama, S.; Yoshida, M.; Asari, T.; Yakushiji, F.; Nishimatsu, S.; Ohsawa, Y.; Itoh, F.; Negishi, Y.; Sunada, Y.; Hayashi, Y. Identification of the minimum peptide from mouse myostatin prodomain for human myostatin inhibition. *J. Med. Chem.* **2015**, *58*, 1544–1549.

(19) Asari, T.; Takayama, K.; Nakamura, A.; Shimada, T.; Taguchi, A.; Hayashi, Y. Structural basis for the effective myostatin inhibition of the mouse myostatin prodomain-derived minimum peptide. *ACS Med. Chem. Lett.* **2017**, *8*, 113–117.

(20) Takayama, K.; Nakamura, A.; Rentier, C.; Mino, Y.; Asari, T.; Saga, Y.; Taguchi, A.; Yakushiji, F.; Hayashi, Y. Effect of N-terminal acylation on the activity of myostatin inhibitory peptides. *ChemMedChem* **2016**, *11*, 845–849.

(21) Takayama, K.; Rentier, C.; Asari, T.; Nakamura, A.; Saga, Y.; Shimada, T.; Nirasawa, K.; Sasaki, E.; Muguruma, K.; Taguchi, A.; Taniguchi, A.; Negishi, Y.; Hayashi, Y. Development of potent myostatin inhibitory peptides through hydrophobic residue-directed structural modification. *ACS Med. Chem. Lett.* **2017**, *8*, 751–756.

(22) Siemensma, A. D.; Weijer, W. J.; Bak, H. J. The importance of peptide lengths in hypoallergenic infant formulae. *Trends Food Sci. Technol.* **1993**, *4*, 16–21.

(23) Sawyer, T. K.; Sanfilippo, P. J.; Hruby, V. J.; Engel, M. H.; Heward, C. B.; Burnett, J. B.; Hadley, M. E. 4-Norleucine, 7-D-phenylalanine- α -melanocyte-stimulating hormone: a highly potent α -melanotropin with ultralong biological activity. *Proc. Natl. Acad. Sci. U. S. A.* **1980**, *77*, 5754–5758.

(24) Rentier, C.; Takayama, K.; Saitoh, M.; Nakamura, A.; Ikegaya, H.; Taguchi, A.; Taniguchi, A.; Hayashi, Y. Design and synthesis of potent myostatin inhibitory cyclic peptides. *Bioorg. Med. Chem.* **2019**, *27*, 1437–1443.